Property and morphology relationships for ternary blends of polycarbonate, brittle polymers and an impact modifier

T. W. Cheng, H. Keskkula and D. R. Paul*
Department of Chemical Engineering and Center for Polymer Research, University of Texas, Austin, TX 78712, USA
(Received 30 January 1991; revised 15 April 1991; accepted 17 April 1991)

Mechanical properties and the morphology of ternary blends of polycarbonate (PC) with a methacrylated butadiene–styrene (MBS) impact modifier and various brittle polymers (BP), like polystyrene (PS), styrene/acrylontrile (SAN) copolymers, and poly(methyl methacrylate) (PMMA), have been investigated. Component pair miscibility, interfacial energies and mixing sequence influence phase morphology and blend properties. Blends prepared by a two-step mixing sequence usually exhibited better properties than those prepared by mixing all components simultaneously. A surface energy analysis is developed for predicting the locus of the MBS particles in the two-phase matrix. This scheme combined with knowledge of pair miscibility proved to be a useful predictive method. It was predicted and found that MBS particles often become trapped at the PC–BP interface by surface forces. Significant toughening of PC blends with PMMA and SAN, but not with PS, was obtained by addition of the MBS impact modifier. For some of the ternary blends, high levels of toughness and reduced notched sensitivity were achieved without any loss of modulus relative to polycarbonate.

(Keywords: blends; polycarbonate; styrenic copolymers; poly(methyl methacrylate) impact modifiers; interfacial energy)

INTRODUCTION

Bisphenol A polycarbonate (PC) is an important engineering polymer used in a wide variety of applications because of its excellent balance of properties including optical clarity, high heat deformation temperature, toughness and electrical properties. However, PC has deficient characteristics that deter its use in some areas. The exceptional toughness it is noted for is not retained in thick moulded sections, when there are sharp notches, at low temperatures and after physical ageing. In addition, it has poor radiation, solvent and hydrolysis resistance. A number of approaches have been used to enhance these end-use properties[1–12]. For example, blends of PC with acrylonitrile–butadiene–styrene (ABS) materials provide products with an improved balance of properties at reduced cost in comparison to that of PC and have been commercially available for some time[1–3,10]. Some recent papers suggest that PC may also be toughened by brittle polymers such as styrene–acrylonitrile (SAN) copolymers[7,11], and poly(methyl methacrylate) (PMMA)[8,12]. In general, one does not expect incompatible blends to produce materials with good properties[2,13]; hence, it is of particular interest to explore such blends more fully.

ABS materials typically contain 10–30 wt% of small (0.1–1 μm) rubber particles in a SAN copolymer (24–30 wt% AN) matrix. The component polymers of ABS are not miscible with PC[1–3,7]. Since ABS is manufactured independently, its composition and morphology are fixed prior to blending with PC. Therefore, the ratio of PC, SAN and rubber phases in the blend are usually not varied independently. The phase morphology of a typical commercially available PC/ABS blend is shown in *Figure 1*. As might be expected, these photomicrographs show that all the rubber particles are in the SAN phase with none located in the PC phase. Independent control of the content of the three components can be achieved by blending a separately produced grafted rubber with SAN copolymer and PC. This raises interesting questions concerning the optimal and actual distribution of the rubber modifier particles between these separate plastic phases. Several recent papers relate to these issues. Hobbs *et al.*[14,15] and Delimoy *et al.*[16] have described the morphology and properties of ternary blends of PC, poly(butylene terephthalate) (PBT), and an impact modifier. For this system, the impact modifier seems to locate preferentially in the PC phase; however, no systematic attempts to alter this by blend preparation protocol are mentioned. Similar issues of distribution are involved in the compounding of fillers (e.g. carbon black, silica, etc.) in elastomer–elastomer blends for control of processing behaviour and vulcanizate physical properties[17–19]. Hess *et al.*[19] demonstrated that carbon black normally locates preferentially in the polybutadiene component of a 50/50 polybutadiene/natural rubber preblend, and that this distribution results in optimum vulcanizate performance. In addition, carbon black transfer during blending has also been reported. The distribution appears to be influenced by factors such as carbon black affinity

*To whom correspondence should be addressed

0032-3861/92/081606-14

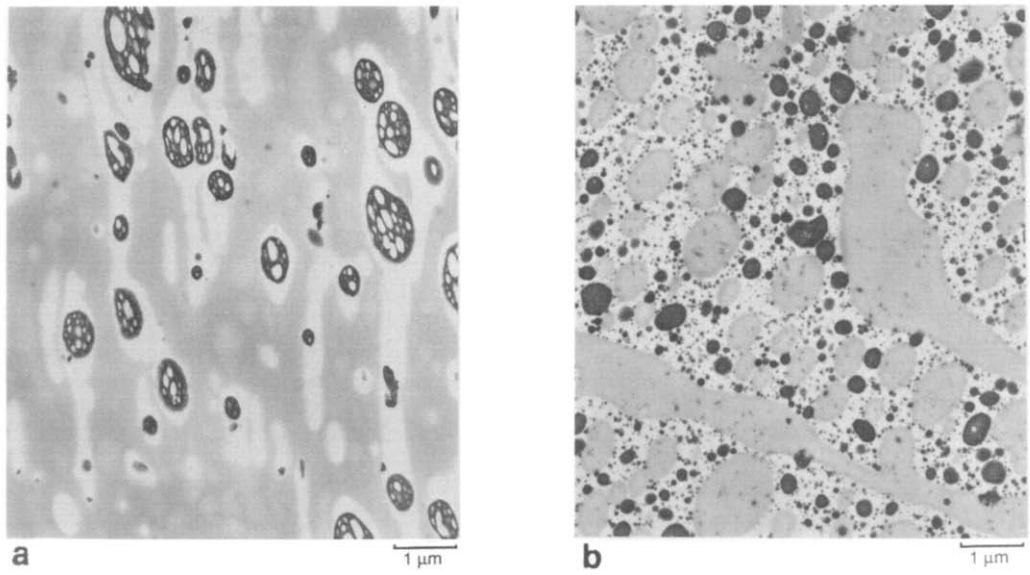

Figure 1 Transmission electron photomicrographs of commercial PC/ABS blends: (a) Pulse 830 (Dow Chemical Co.); (b) Cycoloy C-1950 (General Electric Co.). Darker phase is PC; very small dark particles in both phases are carbon black

for the rubber, blending method, and the relative viscosity levels of the elastomers, etc.[18].

Fowler *et al.*[20] studied the effect of mixing technique and sequence on the distribution of core–shell impact modifier particles, methacrylated butadiene–styrene (MBS) type, in a two-phase polystyrene (PS)/SAN blend and found that the MBS particles had a strong tendency to locate at the PS–SAN interface. In another study, similar MMA grafted particles were found to locate in the interfacial region of a blend of high impact polystyrene (HIPS) and ABS[21]. Binary blends of HIPS and ABS are quite brittle; however, by addition of this MMA grafted elastomer, ternary blends tougher than either HIPS of ABS alone were achieved[21]. It appears that the locus of core–shell modifier particles in two-phase polymer blend matrices may have a significant effect on properties. Accordingly, the purpose of this study is to explore the morphology and properties of ternary blends containing PC, an MBS impact modifier, and one of several brittle polymers (BP) such as PS, SAN and PMMA. In addition, the effects of blending sequence, interfacial forces and thermodynamic affinity on blend phase morphology are examined. These brittle polymers typically have tensile moduli 50–85% higher than PC and thus can add stiffness to mixtures of PC with low modulus impact modifiers.

BACKGROUND

The mechanical properties of binary blends of impact modifiers with a single matrix polymer depend critically on several aspects of the rubber phase morphology such as particle size, uniformity of particle distribution, rubber phase volume, particle size distribution, etc.[21–25]. Rubber toughening of a multiphase matrix polymer introduces distribution of the rubber particles among these phases as a new morphological variable. Recently, Hobbs *et al.*[26] suggested that interfacial forces may play an important role during melt processing in establishing the phase morphology of multiphase polymer blends. The systems used in their study included three- and four-component blends containing PC, PBT, PMMA and various styrenic polymers. They used the concept of a spreading coefficient, λ_{ij}, defined in terms of interfacial tensions, γ_{mn}, via a form of Harkins' equation[27]:

$$\lambda_{31} = \gamma_{12} - \gamma_{32} - \gamma_{13} \quad (1)$$

In a three-phase system, if $\lambda_{31} > 0$, component 3 will have an interfacial driving force to spread over component 1 and eliminate its contact with 2. If λ_{31} and λ_{13} are negative, 1 and 3 will tend to disperse separately in the matrix of 2. Hobbs *et al.* successfully demonstrated the usefulness of the spreading coefficient concept for understanding the morphology of their composites[26]. They had to use various estimation techniques to obtain quantitative values of the appropriate interfacial tensions at the melt processing temperature of 270°C.

The choice of component polymers for this study was based on a number of previous observations. First, a core–shell impact modifier with MMA-based shell was selected because of the near miscibility of PMMA with PC documented in recent papers[12,28,29]. Polystyrene is not miscible with PC or PMMA[22,29–35], while PMMA and SAN are miscible for AN contents between 9 and about 33 wt%[22,30–36]. The lower critical solution temperature, *LCST*, for PMMA blends with SAN vary considerably with the AN content of the latter[35]. An optimum interaction evidently exists in the 13–15% AN range since the *LCST* is so high that it lies above the temperature at which the components degrade. SAN containing 14.7% AN (SAN14.7) was selected to represent this optimum range. Blends containing equal amounts of PMMA and SAN25, on the other hand, phase separate on heating at about 275°C. SAN34 lies just outside the window for miscibility with PMMA. Thus, by choosing PS, SAN14.7, SAN25, SAN34 and PMMA as the brittle polymer (BP) phase along with PMMA grafted rubber particles for the modification of PC, the degree of interaction between the component polymers can be controlled over a considerable range. A number of studies on adhesion between such polymers have appeared[11,13,22,35–38]. Of course, miscible pairs exhibit strong adhesion, particularly when the enthalpic contribution to the free energy of mixing is exothermic[36,39].

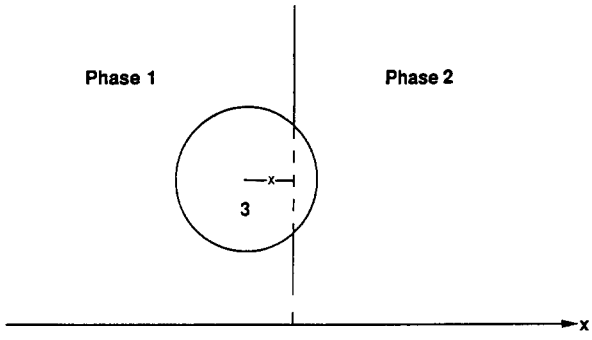

Figure 2 Schematic of a grafted impact modifier particle (3) at a planar interface between polymers 1 and 2

THEORY

Effect of surface forces on equilibrium distribution of modifier particles

The equilibrium location of grafted emulsion modifier particles (component 3) within the two-phase matrix formed by polymers 1 and 2 should, in principle, be determined by interfacial forces of thermodynamic origin. In practice, an equilibrium distribution may not be achieved since kinetic issues could dominate in some circumstances[20]. Particle motions within a phase are probably more influenced by the complex flow fields involved in mixing or fabrication and rheological characteristics than by traditional diffusion and gravity forces that dominate in low viscosity fluids. The purpose here is to analyse more fully the surface thermodynamic effects since this problem is a tractable one. Deviations from the predictions of this approach may be taken as arguments for the importance of other effects like those mentioned above.

The ternary system of interest here is quite analogous to that treated by Hobbs *et al.*[26] except for the following. Here, component 3 is not fluid and retains its original spherical geometry during processing. We assume that it has surface properties characteristic of the polymer that forms the grafted shell which is PMMA in the present case. The simple spreading coefficient analysis described by Hobbs *et al.*[26] is pertinent here, but a more complete surface thermodynamic analysis will prove useful. We begin by considering the surface energy of a particle of 3 that is already interrupting a planar 1–2 interface as shown in *Figure 2*. The surface free energy of this system relative to the uninterrupted 1–2 interface is given by[40,41]:

$$G = A_{13}\gamma_{13} + A_{23}\gamma_{23} - A_{12}\gamma_{12} \qquad (2)$$

where the first two terms on the right-hand side represent the sum of the products of surface energy and surface area contact of particle 3 with phases 1 and 2. The third term reflects the loss of 1–2 contact area and, therefore, surface free energy caused by the presence of 3 at this interface. Thus, A_{12} is a planar area (see dotted line in *Figure 2*) while A_{13} and A_{23} are spherical segments that add up to $4\pi R^2$, where R = radius of particle 3. Assuming the centre of the particle is a distance x from the 1–2 interface and $-R < x < R$, then substitution of geometrical relations for these areas into equation (2) yields:

$$G = 2\pi R^2\left\{\left(1 - \frac{x}{R}\right)\gamma_{13} + \left(1 + \frac{x}{R}\right)\gamma_{23} - \frac{1}{2}\left[1 - \left(\frac{x}{R}\right)^2\right]\gamma_{12}\right\} \qquad (3)$$

This relation reduces to

$$G = 4\pi R^2\gamma_{13} \quad \text{when } x < -R \qquad (4)$$

$$G = 4\pi R^2\gamma_{23} \quad \text{when } x > +R \qquad (5)$$

for the limits shown, as expected.

Figure 3 shows how this surface free energy varies with x within the range $-R \leqslant x \leqslant R$, when 3 is in contact with both 2 and 1, for different relative values of γ_{ij}. The force on 3 resulting from these effects is given by:

$$-\frac{\partial G}{\partial x} = 2\pi R\left[\gamma_{13} - \gamma_{23} - \gamma_{12}\left(\frac{x}{R}\right)\right] \qquad (6)$$

For the case $\gamma_{13} > \gamma_{23}$ shown in *Figure 3*, this force is positive at every point in the range $-R$ to $+R$ when:

$$\gamma_{12} \leqslant \gamma_{13} - \gamma_{23} \qquad (7)$$

In this case, when a particle of 3 in phase 1 approaches the 1–2 interface by some means, there will be a surface force acting to drive it into phase 2. This can be restated in terms of the spreading coefficient defined by Harkins[27]:

$$\lambda_{21} = \gamma_{13} - \gamma_{23} - \gamma_{12} \qquad (8)$$

Thus, according to equation (7), $\lambda_{21} \geqslant 0$ means that species 2 will displace species 1 on a surface of 3. On the other hand, when $\gamma_{23} > \gamma_{13}$, the force acting on the particles will be negative everywhere within $-R$ to $+R$ if:

$$\gamma_{12} \leqslant \gamma_{23} - \gamma_{13} \qquad (9)$$

Similarly, 1 will displace 2 when:

$$\lambda_{12} = \gamma_{23} - \gamma_{13} - \gamma_{12} \geqslant 0 \qquad (10)$$

These limiting cases predict that 3 should reside entirely in phase 2 ($\lambda_{21} \geqslant 0$) or in phase 1 ($\lambda_{12} \geqslant 0$) if surface energy effects dominate.

There will be a position of minimum surface free energy, or zero force, on particle 3 at the 1–2 interface when:

$$\gamma_{12} > \gamma_{13} - \gamma_{23} \qquad (11)$$

as shown in *Figure 3* for $\gamma_{13} > \gamma_{23}$ (or when $\gamma_{12} >$

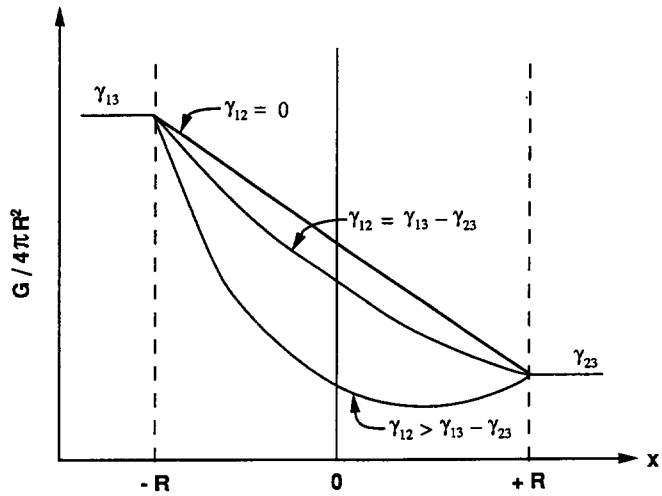

Figure 3 Surface energy when a particle of 3 (radius = R) interrupts a 1–2 interface. Drawn for the special case when $\gamma_{13} > \gamma_{23}$

$|\gamma_{13} - \gamma_{23}|$ in the general case). This position of zero force is located at:

$$\frac{x}{R} = \frac{\gamma_{13} - \gamma_{23}}{\gamma_{12}} \tag{12}$$

Thus, unless other issues dominate, particles of 3 can become trapped at the 1–2 interface by surface forces (i.e. $-1 < x/R < 1$). Since the right-hand side of equation (11) involves a difference of surface energies, this condition seems rather likely to be satisfied. Because the surface energy γ_{ij} reflects the thermodynamic interaction[37] between i and j, it is clear that surface trapping is all the more likely when polymers 1 and 2 have a strong repulsion for each other.

It is interesting to consider what this analysis predicts when the shell of 3 is selected to be miscible with one of the phases, say 2. In this case, we might automatically expect 3 to prefer to reside in phase 2[20]; however, surface trapping may still be possible according to this analysis. When 2 and the shell of 3 are miscible, we expect:

$$\gamma_{23} = 0 \tag{13}$$

but the condition for surface trapping (equation (11)) is still satisfied if:

$$\gamma_{12} > \gamma_{13} \tag{14}$$

However, when the shell of 3 is miscible with 2, the interpenetration of the two types of chains results in other contributions to the free energy that may render this analysis invalid. Furthermore, the entanglement of the chains grafted to the surface of 3 with polymer 2 is likely to involve rheological forces that could make kinetic issues dominant. Thus, the prediction of equation (14) must be viewed with some caution.

Kinetics of particle motion at the interface

As a final issue we consider the kinetics of particle motion near the interface. For simplicity we assume that the resistance to motion is given by Stokes's law[42] and that only surface forces act to move the particle. A force balance leads to:

$$6\pi\mu R \frac{dx}{dt} = 2\pi R\left[\gamma_{13} - \gamma_{23} - \gamma_{12}\left(\frac{x}{R}\right)\right] \tag{15}$$

where μ is the viscosity (assumed to be the same for 1 and 2). This equation can be integrated from $-R$ to $+R$ to find the time:

$$t = \frac{3\mu R}{\gamma_{12}} \ln\left(\frac{\gamma_{13} + \gamma_{12} - \gamma_{23}}{\gamma_{13} - \gamma_{23} - \gamma_{12}}\right) = \frac{3\mu R}{\gamma_{12}} \ln\left(-\frac{\lambda_{12}}{\lambda_{21}}\right) \tag{16}$$

for a particle of 3 to move across the interface from 1 to 2 driven only by the interfacial free energy gradient. This occurs in a finite time provided the condition for trapping (equation (11)) is not satisfied. If we assume $R = 0.2\ \mu m$, $\gamma_{12} = 1 \times 10^{-3}$ N m^{-1}, and $\mu = 1 \times 10^3$ Pa s as typical values, then the characteristic time $3\mu R/\gamma_{12}$ takes on the value 0.6 s. This characteristic time is short relative to the typical residence time in processing equipment which is generally a few minutes; however, it is relatively long compared to the local process time-scale given by the reciprocal of the typical processing shear rate of 10^3 s^{-1}, i.e. 0.001 s. Based on this order of magnitude analysis, one must conclude that equilibrium distribution of particles is possible but not assured.

EXPERIMENTAL

The polymers used in this study and described in *Table 1* are commercially available materials. Ternary blends were prepared from PC as the major component, a brittle polymer, and an impact modifier. The MBS modifier is an emulsion-made MBS core–shell elastomer available from Rohm and Haas Co. as Acryloid KM 680. It contains about 80 wt% of a butadiene-based rubber in the form of 0.18 μm diameter particles that have a PMMA-based outer shell. More details of this rubber modifier have been given elsewhere[22].

Prior to melt processing, PC was dried for a minimum of 24 h at 105°C in an air circulating oven, while the brittle polymers and MBS modifier were dried at 75°C. Melt blending was carried out in a Killion single screw extruder ($D = 2.54$ cm, $L/D = 30$) at 270°C. The single strand extrudate was pulled through a water bath and pelletized. For order of mixing sequences, we use PC/BP/MBS to designate the simultaneous mixing of

Table 1 Details of polymers used

Polymer	Abbreviation	Source (designation)	$\bar{M}_n$	$\bar{M}_w$
Polycarbonate	PC	Dow Chemical Co. (Calibre 300-4)	13400	36000
Poly(methyl methacrylate)	PMMA	Rohm & Haas Co. (Plexiglas V811)	52900	105400
Polystyrene	PS	Cosden Oil and Chemical Co. (550P)	100000	350000
Poly(styrene-*co*-acrylonitrile)				
14.7% AN	SAN14.7	Asahi Chemical Co.	83000	182000
25% AN	SAN25	Dow Chemical Co. (Tyril 1000)	77000	152000
34% AN	SAN34	Asahi Chemical Co.	73000	145000
Methacrylated butadiene–styrene impact modifier	MBS	Rohm & Haas Co. (Acryloid KM 680)	Not applicable	
Pulse[a]		Dow Chemical Co. (Pulse 830)	Not applicable	

[a] A commercial PC/ABS blend

Table 2 Mechanical properties of PC and blends

Material	Yield stress (MPa)	Modulus (MPa)	Elongation at break (%)	Impact strength ($J\ m^{-1}$)	
				Standard notch	Sharp notch
PC	56	2034	>100	940	53
Pulse 830	51	2103	>100	652	543
PC/MBS (7/3)	32	1241	>100	352	294
PC/PS (6/3)	59	2462	80	32	–
PC/SANS14.7 (6/3)	60	2393	>100	59	–
PC/SAN25 (6/3)	63	2476	>100	64	–
PC/SAN34 (6/3)	64	2566	100	48	–
PC/PMMA (6/3)	63	2441	95	59	–
PC/PS/MBS[a]	49	1986	13	123	108
PC/SAN14.7/MBS	50	2110	13	390	363
PC/SAN25/MBS	53	1972	44	464	432
PC/SAN34/MBS	54	2186	28	368	304
PC/PMMA/MBS	52	1931	78	475	368

[a]The composition of all ternary blends is 60/30/10 and they were prepared by simultaneous mixing of all components in a single screw extruder

the three components and BP/MBS + PC, for example, to indicate that the brittle polymer and MBS modifier are blended first followed by addition of PC in a second extrusion step. Thus, the plus sign denotes a second melt mixing step. There are three two-step mixing sequences used here, i.e. BP/MBS + PC, PC/BP + MBS and PC/MBS + BP. The blended pellets were dried at 100°C overnight prior to moulding at 270°C into standard tensile (ASTM-638 type I) and Izod (ASTM-256) bars using an Arburg Allrounder 305 screw type injection moulding machine.

A Barbender Plasti-Corder equipped with a 50 cm^3 sample chamber was used for examining the maximum torque at a rotor speed of 60 rev min^{-1}. A process temperature of 270°C was used.

Tensile properties were determined according to ASTM D-638 using an Instron 1137 with a computerized data acquisition system at a crosshead speed of 0.8 mm min^{-1}. A strain gauge extensometer was used to obtain the modulus and yield properties. Notched Izod impact strengths were measured according to ASTM D-256 using a pendulum type tester. For some samples, a sharp notch was made by cutting smoothly into the centre of the machined notch using a fresh razor blade. A minimum of five bars were used in each test. Standard deviations of 5% or less were found for stress, modulus and notched Izod impact values. The standard deviation for strain at break was found to be 10–20% of the average values.

The morphology of the blends was characterized by transmission electron microscopy using a Hitachi HU11-E. First, specimen blocks were stained in a 2% solution of OsO_4 for at least 48 h. Ultrathin slices were cut using a Reichert-Jung Ultracut Microtome at room temperature. For improved contrast in some cases, the ultrathin sections were further stained by the vapour of a 0.5% RuO_4 solution for a maximum of 15 min[43]. In this study, specimen blocks were cut from the core area of injection moulded bars and microtomed sections were cut perpendicular to the flow direction unless specified otherwise.

MECHANICAL PROPERTIES

In this study, weight ratio of 60% PC, 30% BP and 10% MBS modifier were maintained in most blends, except when specified otherwise, in order to fix the dispersed and continuous phases and to permit unambiguous identification of the components. The ratio of 3/1 for BP/MBS is typical of commercial ABS materials.

Table 2 summarizes the mechanical properties of PC and related binary and ternary blends. In binary blends with PC, the MBS modifier reduces the yield stress and modulus, but blends remain tough, even when a sharp notch is introduced. However, addition of brittle polymers, like PS, SAN and PMMA, increase the yield stress and modulus, but embrittle the blends in all cases. In the ternary blends, obtained by simultaneous mixing, tensile properties are only slightly affected by the presence of MBS particles but impact strength is significantly enhanced for specimens with both standard and sharp notches, relative to binary PC/BP or PC/MBS blends.

The effects of mixing sequence on the mechanical properties of selected blends are shown in *Table 3*. The variations in tensile properties, such as yield stress and modulus, are small, under 3% in general except for the elongation at break. The mixing order BP/MBS + PC gives best results when the BP is PMMA or SAN25, while the order PC/MBS + BP gives best results for PS. The Izod impact strength of specimens with standard and sharp notches, are also shown in *Table 3*. In each case, one of the two-step preparation procedures yields blends with better mechanical properties, including toughness, than those prepared by simultaneous mixing.

A comparison of impact strengths for related binary and ternary blends is shown in *Figure 4*. The binary blends were prepared by two passes through the extruder. For ternary systems, data were chosen from blends prepared by the two-step mixing protocol that gave the best results. When BP is PMMA or SAN25, the ternary blends are tougher than any combination of only two components. In addition, specimens of these ternary blends with sharp notches still fail in a ductile mode. The

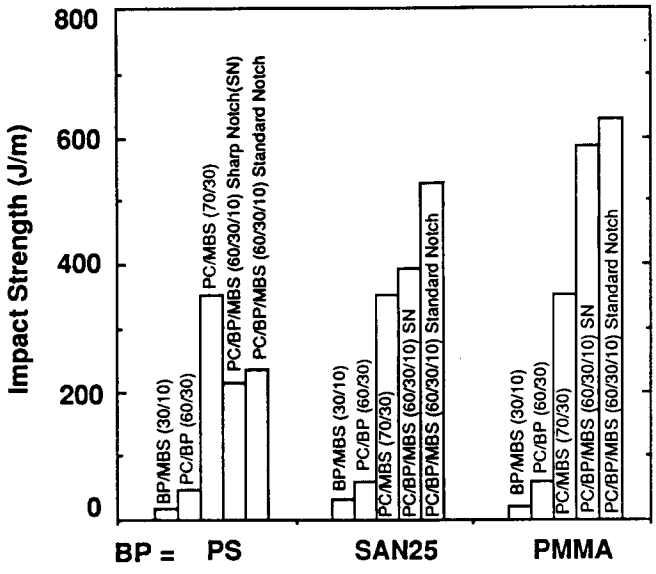

Figure 4 Comparison of impact strength of binary and ternary PC blends. For ternary blends, the data are the optimum obtained from the various two-step mixing protocols used

impact strength of the ternary blend containing PS is relatively low. That is, MBS toughens PC/PMMA and PC/SAN blends but does not appreciably improve the toughness of PC/PS blends.

BLEND MORPHOLOGY

Blends prepared by simultaneous mixing of components

Figure 5a shows a transmission electron photomicrograph of the PC/MBS 80/20 blend. The MBS modifier disperses well so that the original emulsion particles appear discretely in the matrix without significant agglomeration. The size and shape of the monodisperse particles (0.18 μm) remains uniform in the blend. For

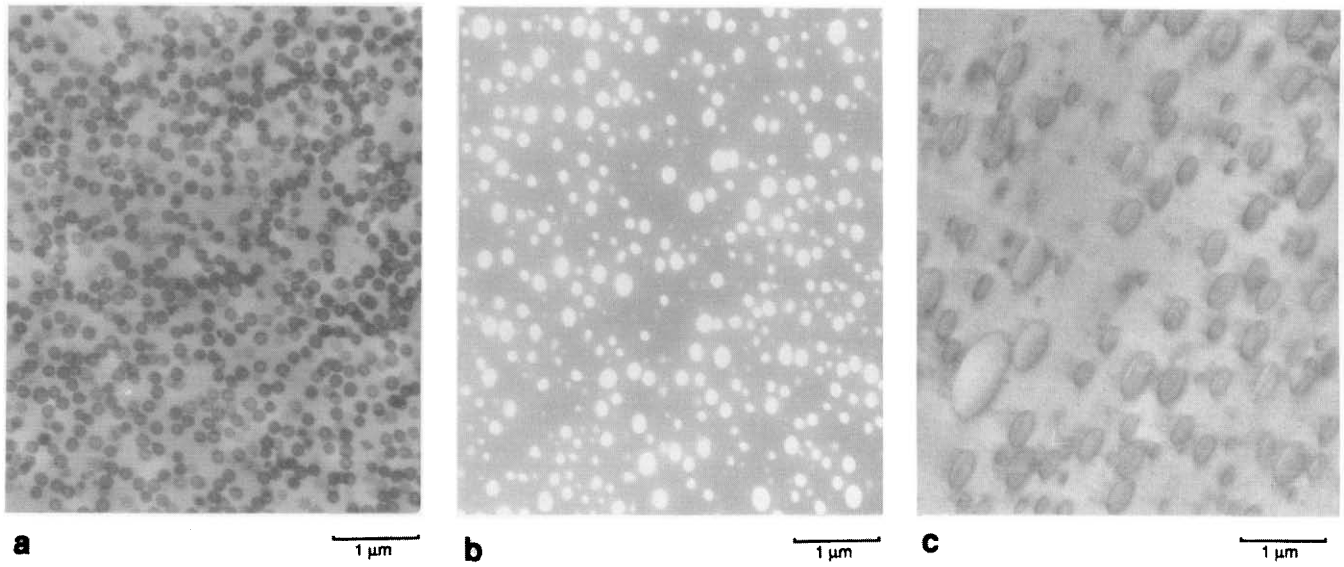

Figure 5 Transmission electron photomicrographs of 80/20 PC blends (perpendicular view): (a) PC/MBS (stained by OsO_4); (b) PC/PMMA (stained by RuO_4); (c) PC/PS (stained by RuO_4)

Table 3 Effect of mixing protocol on mechanical properties of ternary PC blends

Mixing protocol	Yield stress (MPa)	Modulus (MPa)	Elongation at break (%)	Izod impact strength (J m^{-1})	
				Standard notch	Sharp notch
PC/PS/MBS[a]					
PC/BP/MBS[b]	49	1986	13	117	107
BP/MBS + PC[c]	49	1979	25	165	149
PC/BP + MBS	48	1957	11	133	112
PC/MBS + BP	50	1972	90	234	214
PC/SAN25/MBS					
PC/BP/MBS	52	1973	44	464	432
BP/MBS + PC	54	2021	77	630	593
PC/BP + MBS	52	2138	43	496	459
PC/MBS + BP	52	2103	77	448	379
PC/PMMA/MBS					
PC/BP/MBS	53	1931	78	480	368
BP/MBS + PC	53	1958	99	443	342
PC/BP + MBS	53	1896	98	528	390
PC/MBS + BP	52	1917	95	438	320

[a]Composition of all ternary blends is 60/30/10
[b]PC/BP/MBS denotes simultaneous mixing; BP = brittle polymer
[c]Plus sign denotes a second mixing step

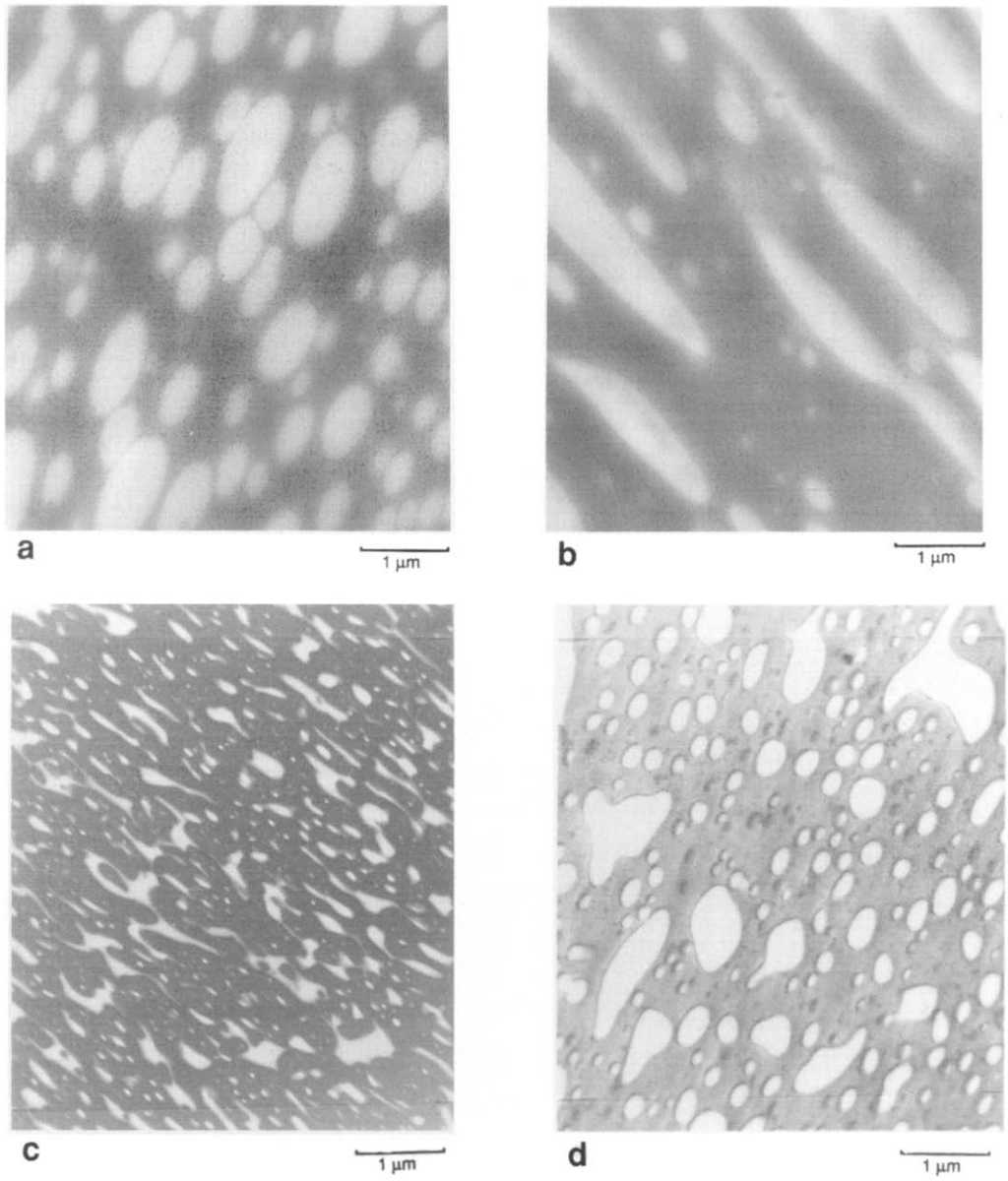

Figure 6 Transmission electron photomicrographs of PC/BP 60/30 blends: (a) PC/PS (perpendicular view, stained by OsO_4); (b) PC/PS (parallel view, stained by OsO_4); (c) PC/PMMA (perpendicular view, stained by RuO_4); (d) PC/SAN25 (perpendicular view, stained by RuO_4)

the BP/MBS blends, similar particle morphologies have been observed for each BP matrix used in this study[20,22]. Blends of PC with each brittle polymer have relatively large domains whose size and shape depend strongly upon composition and processing conditions[44–50]. Generally, for blends containing 20% or less BP, the latter forms spherical dispersed particles[46]. When 80/20 PC/BP blends are viewed perpendicular to the flow direction, those based on PMMA have the smallest domains, average diameter = 0.27 μm, while blends with PS have the largest domains, average diameter = 0.7 μm, as shown in *Figures 5b* and *c*, respectively. Blends with SAN have intermediate domain sizes (0.65 μm). The average diameters quoted were computed from the largest 50 particles in the TEM photomicrograph. *Figure 6* shows that the brittle polymer domains in PC/BP 60/30 blends are oriented due to injection moulding. This orientation is demonstrated in *Figures 6a* and *b* for PC/PS blends. When viewed perpendicular to the flow direction, round and ellipitcal shapes are observed; while parallel to the flow direction, long cigar-shaped domains are observed[46]. PC/PMMA blends tend to show co-continuous domains, while PC/SAN25 blends exhibit intermediate morphology. Similar results have been reported elsewhere[8,44–46].

A series of transmission electron photomicrographs of 60/30/10 ternary blends prepared by simultaneous mixing of the components are shown in *Figure 7*. For the ternary blend containing PMMA (*Figure 7a*), the MBS particles reside entirely in the PMMA phase with no stray particles in the PC (darker) phase. This morphology is reasonable owing to the fact that the graft chains in the MBS shell are chemically identical with those of the PMMA phase. *Figure 7b* shows the morphology of the ternary blend containing PS. The MBS particles are mostly located at the PC–PS interface, while a few of them can be found in the PC (darker) phase. Because of the well dispersed nature of the PS phase, the amount of MBS is not sufficient to cover the entire interfacial area. Photomicrographs of ternary

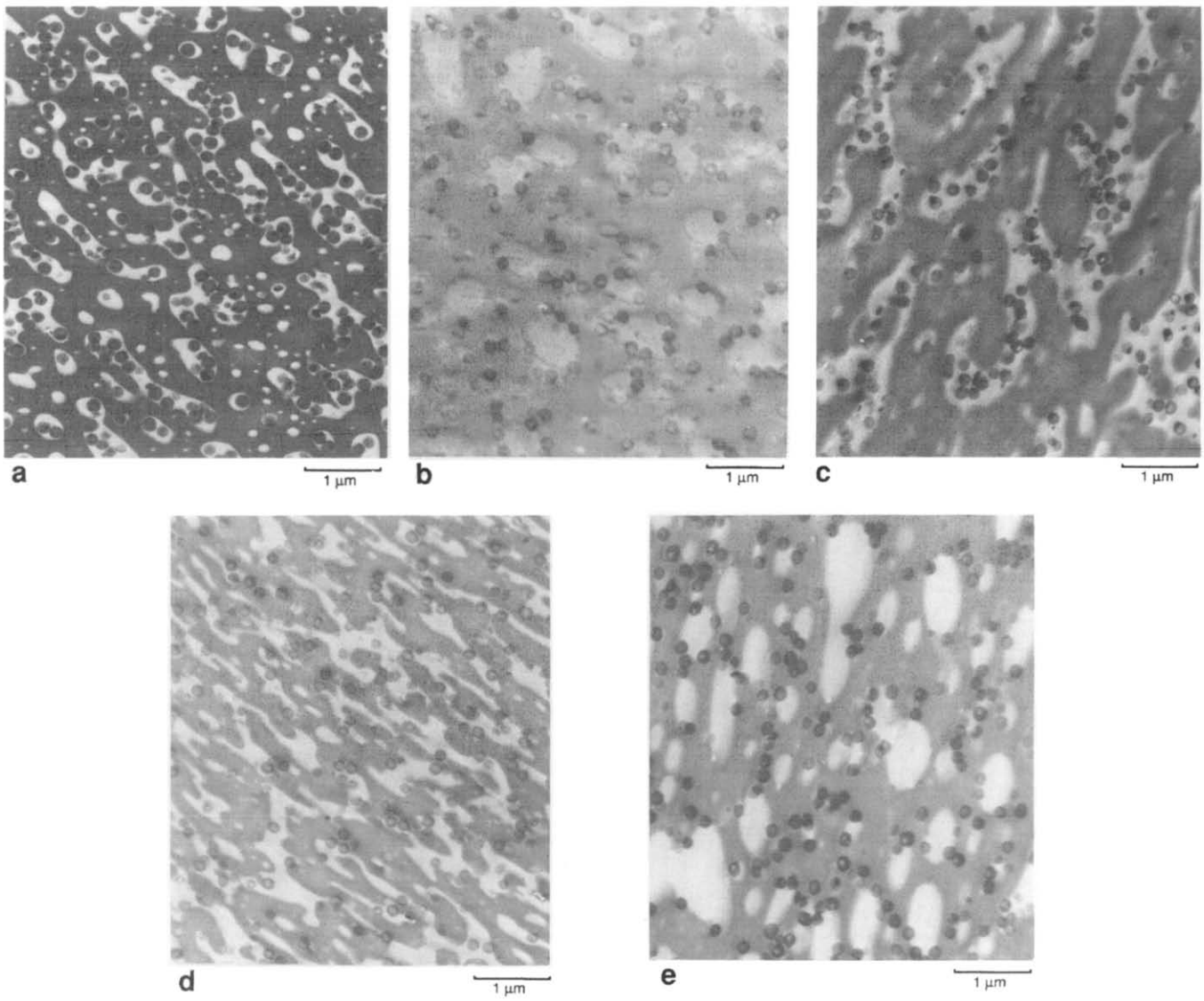

Figure 7 Transmission electron photomicrographs of PC/BP/MBS 60/30/10 blends prepared by simultaneous mixing (perpendicular view, stained by OsO_4 and RuO_4): (a) PC/PMMA/MBS; (b) PC/PS/MBS; (c) PC/SAN14.7/MBS; (d) PC/SAN25/MBS; (e) PC/SAN34/MBS

blends involving the three different SAN copolymers are shown in *Figures 7c* to *e*. In the case of SAN14.7, the PC and SAN phases are co-continuous. This co-continuity does not occur in the absence of the MBS particles (*Figure 6d*). In addition, the MBS particles are completely located in the SAN14.7 phase. This might be expected since PMMA (the shell material of MBS) and SAN14.7 are miscible and have a relatively favourable interaction as judged from the high *LCST*[22,36]. For the ternary blend involving SAN25, the MBS particles tend to be at the PC–SAN25 interface as well as in both the PC and SAN25 phases. Apparently, MBS particles interact sufficiently with both the PC and SAN25 phases to give such morphology. The morphology of ternary blends with SAN34 is similar to that of blends with PS. None of the MBS particles were found in the SAN34 phase. A schematic comparison of binary blend morphology with that of ternary blends prepared by simultaneous mixing is shown in *Figure 8* (views are perpendicular to the flow direction). Generally, for PMMA, SAN14.7 and SAN25 containing ternary blends, the brittle polymer phase seems to be enlarged by adding the MBS modifier and tends toward co-continuity with the PC phase. For ternary blends involving PS and SAN34, however, this phase tends to remain about the same upon addition of MBS. Note that PS and SAN34 are both outside the window of miscibility with PMMA.

Effect of two-step mixing sequence

It has been found that the sequence of mixing has a significant influence on the location of MBS particles in PS/SAN blends[20]. As mentioned, four different mixing sequences have been used in this study. During processing, the various process variables such as temperature, pressure, screw speed and composition were kept constant for all blends.

In the ternary blends involving PMMA, the MBS particles reside in the PMMA phase in all cases. Blending sequence has no discernable effect on the morphology of this system.

TEM photomicrographs of 60/30/10 ternary blends involving PS are shown in *Figure 9*. Generally, the MBS particles are at the PC–PS interface. Some particles are also found in the PC phase, but none in the PS phase. For the sequences PS/MBS + PC (*Figure 9b*) and

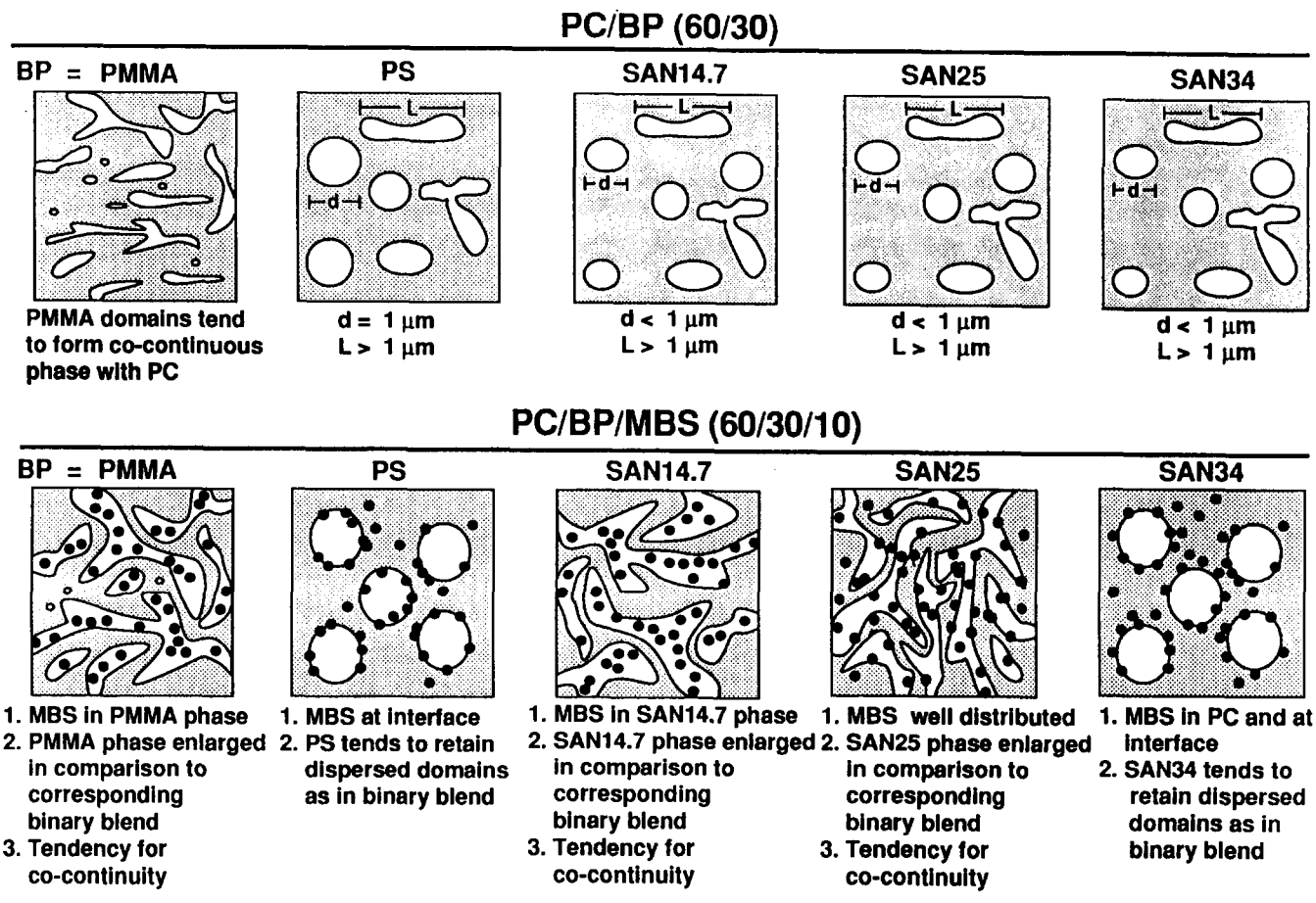

Figure 8 Schematic comparison of morphology of binary and ternary blends

PC/MBS + PS (*Figure 9d*), PC and PS tend to form co-continuous phases compared to the sequences PC/PS/MBS (*Figure 9a*) and PC/PS + MBS (*Figure 9c*). As summarized in *Table 2*, blends prepared by the former two methods show better ductility as indicated by Izod impact strength and elongation at break. Since blending sequences affect the phase morphology of ternary blends containing PS, there is a corresponding influence on blend properties.

Figure 10 shows photomicrographs for 60/30/10 ternary blends involving SAN25 prepared by the four different methods. The presence of MBS particles causes a trend toward co-continuity of PC and SAN25 in all cases. Although the MBS particles are relatively well distributed, they are more likely to align at the PC–SAN25 interface. This is especially true when the PC–SAN25 interface is established prior to adding the MBS particles, i.e. the mixing sequence designated PC/SAN25 + MBS (*Figure 10c*). The blending sequence MBS/SAN25 + PC (*Figure 10b*) results in more MBS particles in the SAN25 domains than found with other methods. Similarly, more MBS particles are found in the PC phase when the sequence PC/MBS + SAN25 is used (*Figure 10d*).

Role of surface energies and miscibility

The purpose here is to comment on the observed locations of the MBS particles in the various mixed matrices of PC and BP described above in terms of thermodynamic considerations, namely pair surface energies or miscibility. Hobbs *et al.*[26] summarized information from the literature for estimating the interfacial tensions at 270°C of the immiscible polymer pairs of interest here (see *Table 4*). The conclusions reached are, of course, limited by the accuracy of these estimates. Numerous theories[37] provide a direct linkage between the interfacial tension and the thermodynamic polymer–polymer interaction energy for the case of positive interaction parameters that are applicable for immiscible pairs. If components i and j are known to be completely miscible at 270°C, then γ_{ij} is set to zero. We assume that the surface of the MBS particles has properties like that of PMMA. We arbitrarily identify the components as follows BP = 1, PC = 2 and MBS = 3, except for the latter entry in *Table 4*. Thus, unlike the example shown in *Figure 3*, γ_{13} may not always be greater than γ_{23}. The value of the ratio $(\gamma_{13} - \gamma_{23})/\gamma_{12}$ determines the equilibrium location of the MBS particles if the surface energy analysis developed above prevails (see, for example, equation (12)). Except for two cases, this ratio is between -1 and $+1$, which implies that at equilibrium the particles should be trapped at the interface between phases 1 and 2. When BP = PMMA, the MBS particles are marginally predicted to reside in the PMMA phase, whereas when BP = SAN34, the MBS particles are clearly expected to locate in the PC phase.

The last column of *Table 4* summarizes the experimental observations shown in *Figure 7* and elsewhere[20] for the case of simultaneous mixing of the three components.

When BP = PMMA, the surface energy criterion marginally predicts that the MBS particles should reside in the BP phase. When all three components are mixed simultaneously, the MBS particles appear to locate entirely in the PMMA phase which intuitively is

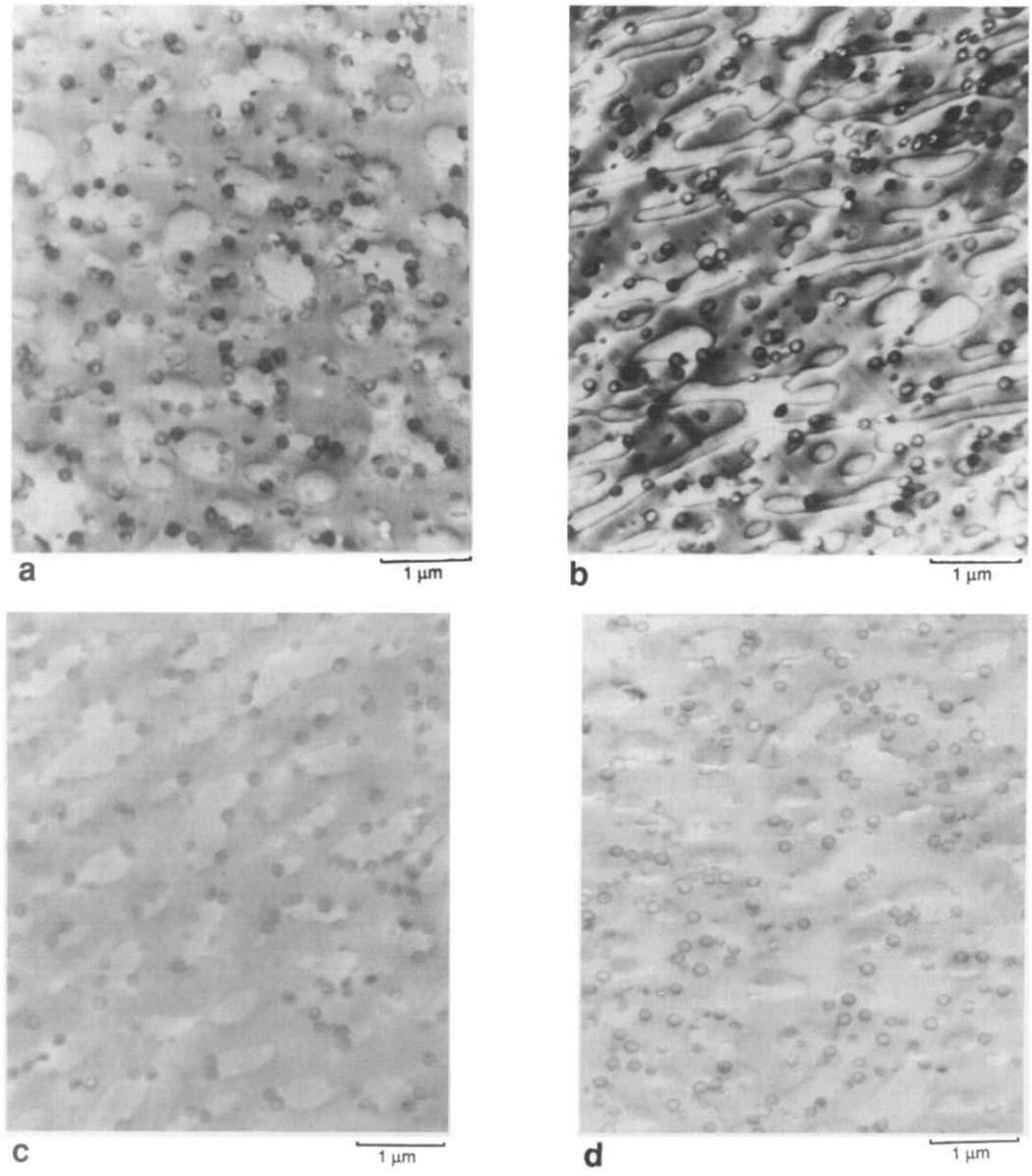

Figure 9 Transmission electron photomicrographs of 60/30/10 ternary blends involving PS prepared by the methods indicated (perpendicular view, stained by OsO_4 and RuO_4): (a) PC/PS/MBS; (b) PS/MBS + PC; (c) PC/PS + MBS; (d) PC/MBS + PS

Table 4 Morphology prediction from analysis of surface forces

PC/BP/MBS blend			Interfacial tensions at 270°C ($\times 10^{-3}$ N m^{-1})			$\frac{\gamma_{13}-\gamma_{23}}{\gamma_{12}}$	Spreading coefficients ($\times 10^{-3}$ N m^{-1})		Morphology	
Particles	Matrix phases								Expected MBS locus	Experimental result[a]
3	1	2	γ_{13}	γ_{23}	γ_{12}		λ_{21}	λ_{12}		
MBS	PMMA	PC	0.00[b]	0.17	0.17	−1.00	−0.34	0.00	MBS in PMMA (marginally)	MBS in PMMA
MBS	PS	PC	0.39	0.17	0.82	0.27	−0.65	−1.04	Trapped at 1–2 interface	Trapped at 1–2 interface Some in PC
MBS	SAN14.7	PC	0.00[b]	0.17	0.45	−0.38	−0.62	−0.28	Trapped at 1–2 interface	MBS in SAN14.7
MBS	SAN25	PC	0.00[b]	0.17	0.48	−0.35	−0.65	−0.31	Trapped at 1–2 interface	Trapped at 1–2 interface Some in both PC and SAN25 phases
MBS	SAN34	PC	1.10	0.17	0.66	1.40	+0.27	−1.59	MBS in PC	MBS in PC and trapped at 1–2 interface
MBS	PS	SAN25	0.39	0.00[b]	0.68	0.57	−0.29	−1.07	Traped at 1–2 interface	Trapped at 1–2 interface[c]

[a] Results are based on samples prepared by simultaneous blending
[b] γ_{ij} set to zero since i and j are miscible
[c] Result reported by Fowler *et al.*[20]

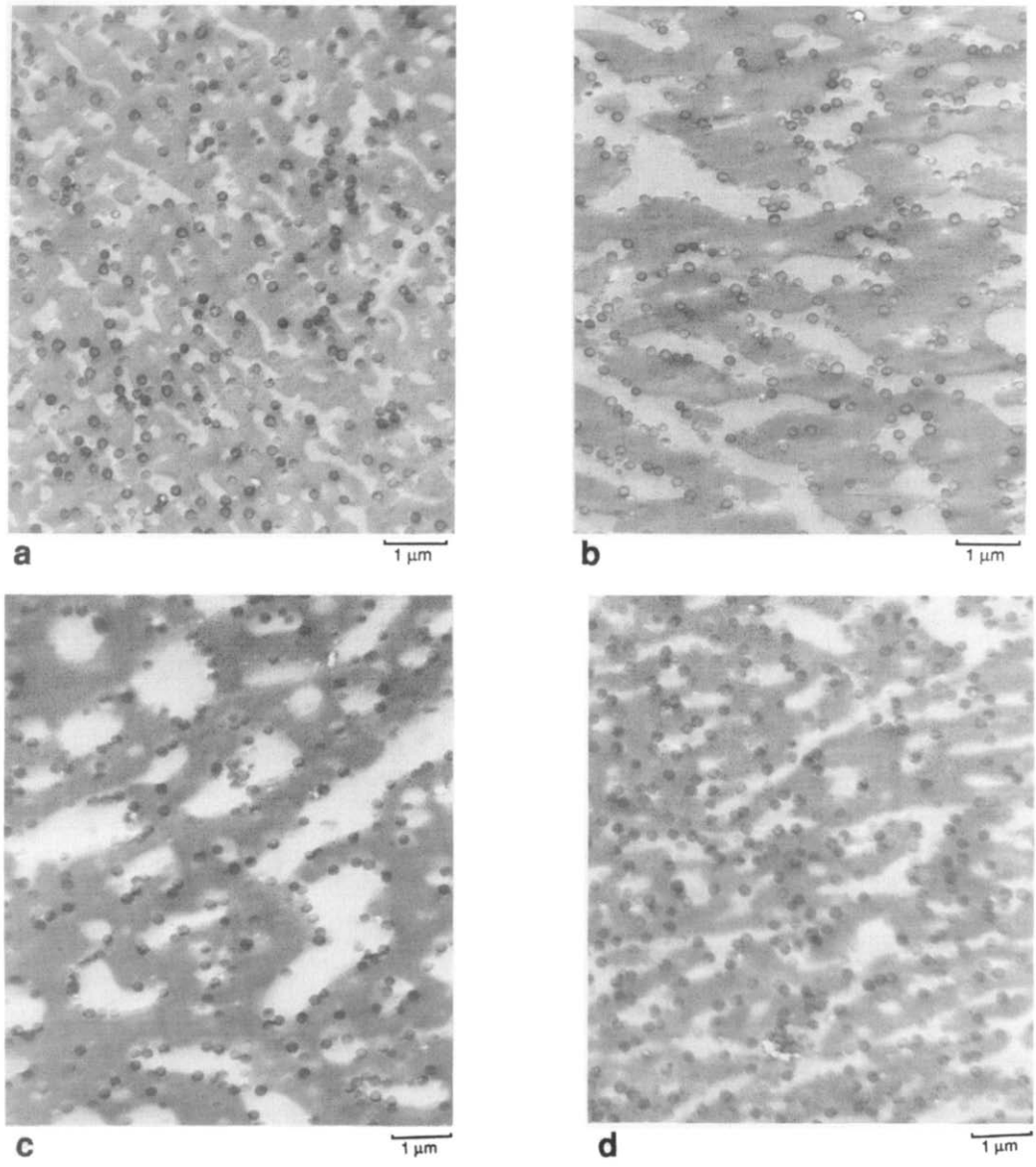

Figure 10 Transmission electron photomicrographs of 60/30/10 ternary blends involving SAN25 prepared by the methods indicated (perpendicular view, stained by OsO_4 and RuO_4): (a) PC/SAN25/MBS; (b) SAN25/MBS + PC; (c) PC/SAN25 + MBS; (d) PC/MBSSAN25

reasonable since the graft chains on the particle surface are chemically identical (hence miscible) with those of the PMMA phase. It should be noted that the PMMA domains are very small and are perturbed by the presence of the MBS particles. Two-step mixing sequences show similar results.

For BP = PS, the MBS particles are predicted to be trapped at the PC–PS interface, and most are (with a few in the PC phase) when simultaneous mixing is used. In addition, MBS particles trapped at the interface appear to be the dominant morphology for blends prepared by two-step mixing protocols.

In the case BP = SAN14.7, the surface energy analysis predicts that MBS particles are trapped at the PC–SAN14.7 interface; however, by simultaneous mixing the MBS particles appear to reside entirely within the SAN14.7 phase. PMMA and SAN14.7 are miscible and should have an exothermic heat of mixing, and earlier we cited reasons why a surface energy analysis might not apply in such cases. Similar morphologies have been observed for blends prepared by two-step mixing protocols.

When BP = SAN25, the surface energy criterion predicts that MBS particles will be trapped at the PC–SAN25 interface. For simultaneous mixing, many of the MBS particles are at the interface but there are some in both the PC and SAN25 phases. Note that SAN25 and PMMA blends are misicible but near the point of phase separation at 270°C. The heat of mixing is no doubt considerably less favourable than for the SAN14.7 case. The SAN25 phase seems more enlarged by two-step mixing, but MBS modifier trapped at the PC–SAN25 interface is still the major morphology for the dispersed particles, especially for the blend prepared by the mixing sequence PC/SAN25 + MBS.

The surface energy analysis prediction when BP = SAN34 is that MBS particles should reside in the PC phase. Note that at 270°C, SAN34 and PMMA are not miscible. For simultaneous mixing, many MBS particles are in the PC phase but a large fraction seems to be at the PC–SAN34 interface. Two-step mixing gave similar results.

Fowler *et al.*[20] reported that MBS particles have a strong propensity to be trapped at the interface in

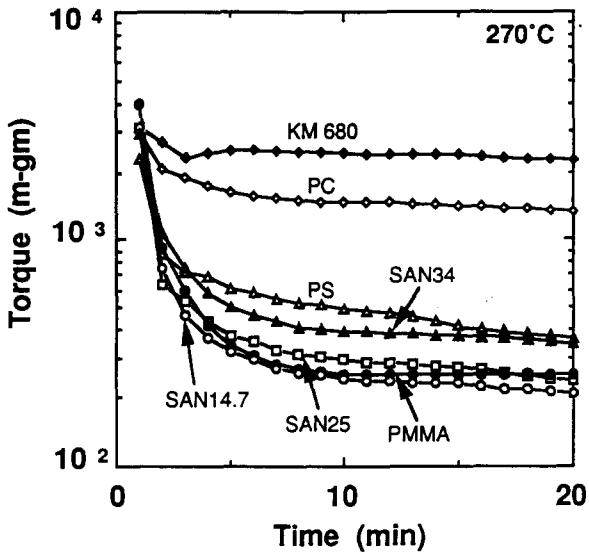

Figure 11 Barbender torque response for individual components at 270°C and 60 rev min^{-1}

PS/SAN25 blends, and this is what the surface energy analysis predicts, as shown in *Table 4*. When blends prepared by the mixing sequence PS/SAN25 + MBS, all of the MBS particles were located in the SAN25 phase. This is, in thermodynamic terms, because the MBS particles have a greater affinity for SAN25 than for PS.

The experiments reported here and elsewhere[20] show that the location of MBS particles in ternary blends is affected by mixing procedure and possibly kinetic issues; however, as shown in the above discussion there is a strong tendency for the particles to assume their equilibrium location based on considerations of surface energies and miscibility of the components. There is strong experimental and theoretical evidence for trapping at the interface in mixed matrices.

Role of rheology

It is well known that rheological properties influence the morphology of immiscible blends, especially domain size[48,51,52]. *Figure 11* shows the comparative rheological properties of the individual components of interest here as determined by torque rheometry. The pure MBS is very viscous as expected since its flow units are entire emulsion particles. Of the matrix materials, PC is the most viscous at the processing temperature used. The viscosities of the other matrices rank in the order PS > SAN34 > SAN25 > PMMA > SAN14.7. Addition of MBS particles to the matrix phases will increase their effective viscosity and possibly alter the ternary morphology relative to the binary morphology because of the change in relative viscosities of the matrix phases. The fact that PC is the major component but each BP has a lower viscosity no doubt contributes to the formation of dispersed phase particles with complex geometry and the tendency for co-continuity of the matrix phases. Of course, the interfacial tension γ_{12} (see *Table 4*) or the effective change in the interface by the presence of MBS particles are other factors that must be considered.

When BP = PMMA, SAN14.7 or SAN25, these phases tend to become larger in ternary blends than they were in the corresponding binary blends without MBS (see *Figures 6* and *7*). One possible reason is that MBS particles tend to locate in these phases which makes them effectively more viscous. On the other hand, for BP = PS and SAN34, these phases are about the same size in ternary blends as in the binary blends without MBS (see *Figures 6* and *7*). MBS particles do not tend to locate in these polymers so their viscosities are not altered.

As discussed earlier, the fact that the location of the impact modifier particles depends to some extent on processing history suggests that equilibrium distribution is not always achieved and that rheological factors no doubt have some role in the actual distribution. Furthermore, we have reported in a separate study[53] that significant morphological changes occur when these three-component blends are melt annealed at 270°C for even very short periods of time. Accordingly, melt morphology that develops during injection moulding is dependent on processing variables. It should be pointed out, however, that the mechanical properties of these blends are not strongly affected by the use of various mixing protocols (*Table 3*).

CONCLUSIONS

The mechanical properties and especially the toughness of ternary blends like those described here depend on many factors including morphology at all levels, interfacial adhesion between component pairs, the inherent toughness or fracture characteristics of each matrix component and, of course, the chemical and physical nature of the modifier. The latter has been held fixed in this work while many of the others have been intentionally varied, although not necessarily individually owing to certain interrelationships that inherently exist. The inability to change only one issue at a time can compromise development of unambiguous conclusions; however, as shown here the current results can be used to obtain numerous useful insights about mechanical behaviour of such blends.

Blends involving the series of SAN copolymers form an interesting set for examining several issues. *Figure 12* shows the impact strength (standard notch) of binary blends and ternary blends (formed by simultaneous mixing of all components) involving this series plotted *versus* the AN content of the SAN. Both sets of blends

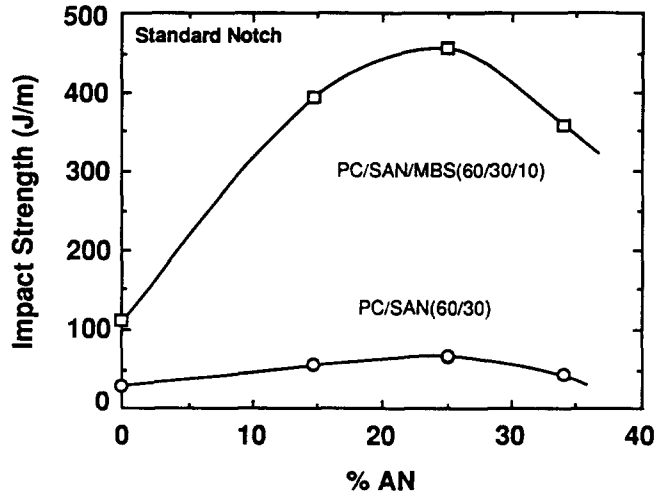

Figure 12 Comparison of Izod impact strength between PC/SAN 60/30 and PC/SAN/MBS 60/30/10 blends prepared by simultaneous mixing

Table 5 Relations between mixing protocol, morphology and impact strength for PC/SAN25/MBS 60/30/10 blends

Mixing protocol	MBS distribution (%)			Impact[a] strength ($J\ m^{-1}$)
	in PC	in SAN25	at PC–SAN25 interface	
PC/BP/MBS	35	5	60	464
BP/MBS + PC	15	25	60	630
PC/BP + MBS	5	5	90	496
PC/MBS + BP	55	5	40	448

[a]Standard notch

appear to have maximum toughness at about 25% AN. Several important issues are influenced by varying the AN content. First, the inherent ductility or the ability to toughen SAN steadily increases from that of PS as the AN percentage increases[54]. While this is no doubt a factor in the general upward trend seen in *Figure 12*, it alone would not suggest that an optimum AN level should exist. Second, the interaction of the PMMA shell of the MBS particles with SAN is most strongly favourable at about 14.7%, and presumably MBS adhesion to and dispersion in this SAN matrix will be at a maximum. While ternary blends involving SAN14.7 are quite tough, those containing SAN25 are tougher. Third, previous work[11] has shown that SAN adhesion to PC is greatest at about 25% AN. Thus, it is tempting to attribute the optimum in toughness for both binary and ternary blends seen in *Figure 12* to this interfacial effect. However, the estimates in *Table 4* suggest that the interfacial energy between PC and SAN copolymers is lower at 14.7% than at 25%.

The location of the MBS particles also affects blend mechanical properties; this can most readily be demonstrated by comparing the ternary blends involving SAN25 prepared by different mixing protocols. *Table 5* shows that premixing SAN25 with MBS prior to blending with PC maximizes the content of MBS in the SAN phase and this blend has the maximum toughness. It seems reasonable that the impact modifier should be located in the brittle polymer in order to achieve a toughened ternary blend.

It is interesting to note that most of the ternary blends described here have greatly diminished notch sensitivity, relative to PC, and therefore higher levels of useful toughness. This is accomplished without sacrificing modulus, i.e. the ternary blends have tensile moduli equal to or higher than that of pure PC. Using optimal mixing protocols, the ternary blends with SAN25 have a balance of mechanical properties fully equivalent to a commercial PC/ABS blend (see *Tables 2* and *3*).

It is important to note that several of the ternary blends described here have higher levels of toughness than any binary combination of the three components, as illustrated in *Figure 4*. It would be most interesting to investigate the origin of this synergism by a detailed study of the fracture mechanism of these materials.

These results show that considerations of surface energy and component pair miscibility can be used to predict the location of impact modifier particles in mixed materials with reasonably good success. Location of particles at the matrix interface is very likely. Mixing protocol plays an important role in determining the locus of these particles in some cases while it has little influence in others. In the systems studied here, the MBS particles are always located in the PMMA or SAN14.7 phases and are not found in the PS or SAN34 phases, regardless of the mixing sequences used. The distribution of MBS particles in PC/SAN25 blend is significantly affected by the mixing method. Note that the chains which form the shell on MBS particles are miscible with PMMA and SAN14.7, immiscible with PS and SAN34, and right on the edge of miscibility with SAN25 at the processing temperature.

ACKNOWLEDGEMENT

This material is based in part on work supported by the Texas Advanced Technology Program under grant no. 066. The authors wish to thank R. S. Schechter for useful discussions on the interfacial energy analysis.

REFERENCES

1 Freitag, D., Grigo, U., Muller, P. R. and Nouvertne, W. in 'Encyclopedia of Polymer Science and Engineering' (Eds H. F. Mark, N. M. Bikales, C. G. Overberger and G. Menges) 2nd edn, John Wiley, New York, 1988, Vol. 11, p. 648
2 Paul, D. R., Barlow, J. W. and Keskkula, H. in 'Encyclolpedia of Polymer Science and Engineering' (Eds Mark Bikales Overberger Menges) 2nd edn, John Wiley, New York, 1988, Vol. 12, p. 399
3 Keskkula, H. and Pettis, A. A. US Patent 3 239 582, assigned to Dow Chemical Co., 8 March 1966
4 Liu, P. Y. and Rosenquint, N. R. US Patent 4 456 725, assigned to General Electric Co., 26 June 1984
5 Liu, P. Y. US Patent 4 390 657, assigned to General Electric Co., 28 June 1983
6 Liu, P. Y. US Patent 4 263 415, assigned to General Electric Co., 21 April 1981
7 Kurauchi, T. and Ohta, T. *J. Mater. Sci.* 1984, **19**, 1699
8 Koo, K. K., Inoue, T. and Miyasaka, K. *Polym. Eng. Sci.* 1985, **25**(12), 741
9 Ferguson, L. E. *Plast. Compounding* 1978, **1**(2), 58
10 Suarez, H., Barlow, J. W. and Paul, D. R. *J. Appl. Polym. Sci.* 1984, **29**, 3253
11 Keitz, J. D., Barlow, J. W. and Paul, D. R. *J. Appl. Polym. Sci.* 1984, **29**, 3131
12 Nishimoto, M., Keskkula, H. and Paul, D. R. *Polymer* 1991, **32**, 1274
13 Paul, D. R. in 'Polymer Blends' (Eds D. R. Paul and S. Newman), Academic Press, New York, 1978, Ch. 12
14 Hobbs, S. Y., Dekkers, M. E. J. and Watkins, V. H. *J. Mater. Sci.* 1988, **23**, 1219
15 Dekkers, M. E. J., Hobbs, S. Y. and Watkins, V. H. *J. Mater. Sci.* 1988, **23**, 1225
16 Delimoy, D., Bailly, C., Devaux, J. and Legras, R. *Polym. Eng. Sci.* 1988, **28**(2), 104
17 Marsh, P. D., Voet, A., Price, L. D. and Mullens, T. J. *Rubber Chem. Technol.* 1968, **41**, 344
18 Corish, P. J. and Powell, B. D. W. *Rubber Chem. Technol.* 1974, **47**, 481
19 Hess, W. M., Scott, C. E. and Callan, J. E. *Rubber Chem. Technol.* 1967, **40**, 371
20 Fowler, M. E., Keskkula, H. and Paul, D. R. *J. Appl. Polym. Sci.* 1989, **37**, 225
21 Keskkula, H., Paul, D. R., McCreedy, K. M. and Henton, D. E. *Polymer* 1987, **28**, 2063
22 Fowler, M. E., Keskkula, H. and Paul, D. R. *Polymer* 1987, **28**, 1703
23 Bucknall, C. B. 'Toughened Plastics', Applied Science Publishers, London, 1977
24 Bucknall, C. B., Davies, P. and Partridge, I. K. *J. Mater. Sci.* 1987, **22**, 1341
25 Hobbs, S. Y. 'Plastic Polymer Science and Technology', (Ed. M. D. Baijal), Wiley Interscience, New York, 1982, Ch. 6
26 Hobbs, S. Y., Dekkers, M. E. J. and Watkins, V. H. *Polymer* 1988, **29**, 1589
27 Harkins, D. W. 'The Physical Chemistry of Surface Films', Reinhold, New York, 1952, p. 23

28 Min, K. E. and Paul, D. R. *J. Appl. Polym. Sci.* 1989, **37**, 1153
29 Saldanha, J. M. and Kyu, Y. *Macromolecules* 1987, **20**, 2840
30 Stein, V. D. J., Illers, R. H. and Henders, H. *Angew. Makromol. Chem.* 1974, **36**, 89
31 Morawetz, H. *Ann. N.Y. Acad. Sci.* 1981, **366**, 404
32 McMaster, L. P. *Adv. Chem. Ser.* 1975, **142**, 43
33 Bernstein, R. E., Cruz, C. A., Paul, D. R. and Barlow, J. W. *Macromolecules* 1977, **10**, 681
34 Naito, K., Johnson, G. E., Allara, D. L. and Kwei, T. K. *Macromolecules* 1978, **11**, 1260
35 Fowler, M. E., Barlow, J. W. and Paul, D. R. *Polymer* 1987, **28**, 1177
36 Fowler, M. E., Barlow, J. W. and Paul, D. R. *Polymer* 1987, **28**, 2145
37 Wu, S. 'Polymer Interface and Adhesion', Marcel Dekker, New York, 1982
38 Barlow, J. W. and Paul, D. R. *Polym. Eng. Sci.* 1984, **24**, 525
39 Park, I., Barlow, J. W. and Paul, D. R. *Polymer* 1990, **31**, 2311
40 Neumann, A. D. 'Wetting, Spreading and Adhesion' (Ed. J. F. Puddy), Academic Press, London, 1978
41 Schechter, R. S., personal communication, 1990
42 Bird, R. B., Stewart, W. E. and Lightfoot, E. N. 'Transport Phenomena', John Wiley, New York, 1960, p. 59
43 Trent, J. S., Scheinbeim, J. I. and Couchman, P. R. *Macromolecules* 1983, **16**, 589
44 Takahashi, H., Matsuoka, T., Ohta, T., Fukumori, K., Kurauchi, T. and Kamigaito, O. *J. Appl. Polym. Sci.* 1988, **36**, 1821
45 McLaughlin, K. W. *Polym. Eng. Sci.* 1989, **29**, 1560
46 Kunori, T. and Geil, P. H. *J. Macromol. Sci.-Phys.* 1980, **B18**(1), 93
47 Berger, L. L. and Kramer, E. J. *J. Mater. Sci.* 1987, **22**, 2739
48 Favis, B. D. and Chalifoux, J. P. *Polym. Eng. Sci.* 1987, **27**, 1591
49 Favis, B. D. and Chalifoux, J. P. *Polymer* 1988, **29**, 1761
50 Favis, B. D. *J. Appl. Polym. Sci.* 1990, **39**, 285
51 Wu, S. *Polym. Eng. Sci.* 1987, **27**, 335
52 Han, C. D. 'Rheology in Polymer Processing', Academic Press, New York, 1976
53 Cheng, T. W., Keskkula, H. and Paul, D. R. *J. Appl. Polym. Sci.* in press
54 Kim, H., Keskkula, H. and Paul, D. R. *Polymer* 1991, **32**, 2372